# Supplementary Material

### 1. Rainfall Spatial Heterogeneity of $\delta^{18}O$

Discerning the rainfall spatial heterogeneity is an important issue as using the water isotopic tracer for transit time evaluation, particularly in meso-scale catchments. Here, we checked the rainfall spatial heterogeneity of event 2 and event 3 in terms of the rainfall amount and its isotopic composition. The spatial distribution of rainfall amount of each storm was interpolated via inverse distance weighted method (power parameter is 2) using data from 4 CWB rain gauges (see Figure 1 in main text). The relative difference (RD) and the coefficient of variation (CV) were calculated for illustrating the spatial heterogeneity (Figure S1 and Table S1). Note that RD was defined as the rainfall minus the average rainfall of a specific cell divided by the mean rainfall of the entire catchment. In this figure, the CVs of the total rainfall are 16% and 10%, respectively, for event 2 and 3 (Figure S1a,b). Such low CVs indicate that the variation is much less than the mean, showing the rainfall spatial pattern is relatively homogeneous. Additionally, the distribution of RD shows that the western part receives more rainfall and the RD has a variation of approx. ±40% of the average. In sum, both indicators show that typhoon-induced rainfall is short-lived, intense, but its rainfall spatial heterogeneity in a meso-scale catchment is not large.

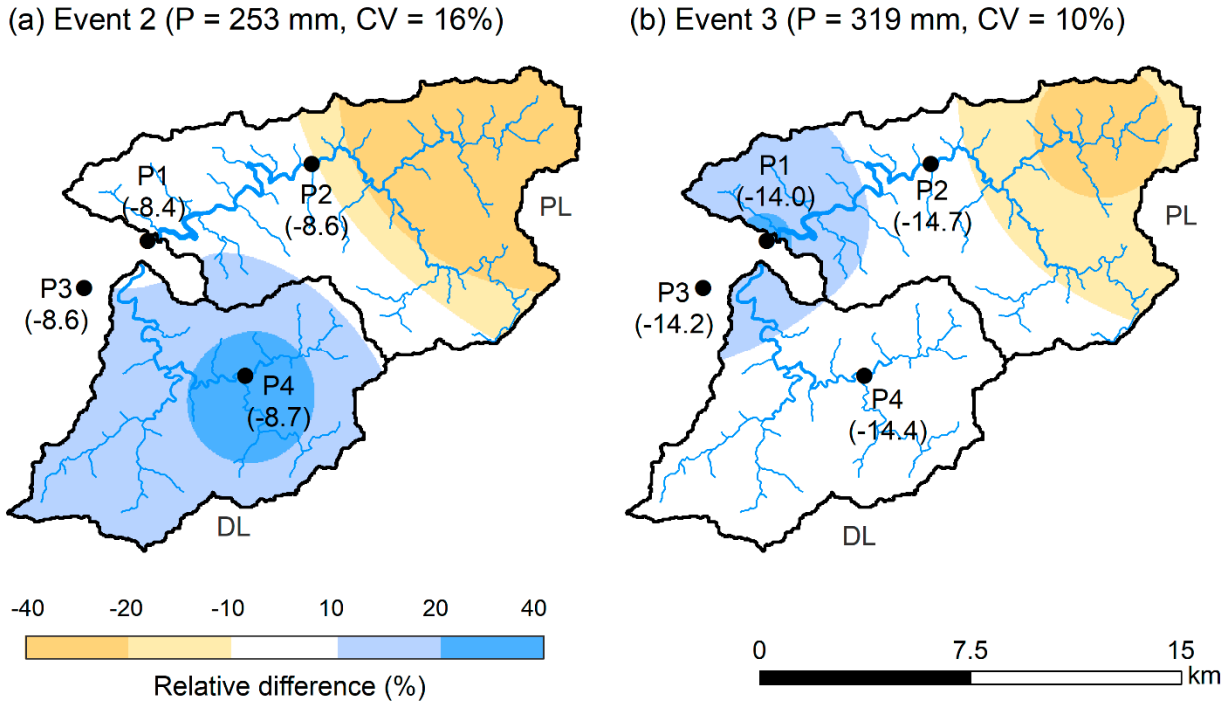


**Figure S1.** Rainfall spatial heterogeneity of event 2 (a) and event 3 (b). The black dots are rainwater sampling sites with $\delta^{18}O$ value in the parentheses.

We further checked the isotopic composition of rainwater during event 2 and 3. The four sampling sites locate in the catchment evenly (Figure S1). Rain sampling site P1 is close to the streamwater sampling site, so rainwater samples were taken every three hours continuously. On the other hand, we also set three remote sampling sites (P2, P3, and P4) to collect rainwater in bulk for the typhoon period. The isotopic compositions of rainwater are shown in Table S1 and Figure S1. The differences of $\delta^{18}O$ values between the 4 sites are less than 0.7‰. Theoretically, $\delta^{18}O$ would be gradually depleted with the increase of altitude. In fact, the strong convective circulation and torrential rainfall brought by typhoons overwhelms the altitude effect. As a result, the isotopic composition of typhoon rainwater is rather consistent. Our results show a low spatial heterogeneity of rainwater isotopic composition.

**Table S1.** The altitude, rainfall, and $\delta^{18}O$ at the rainwater sampling sites (also for model input).

| Gauge ID | Sampling type | Altitude (m) | Event 2 | | Event 3 | |
|---|---|---|---|---|---|---|
| | | | Rain (mm) | $\delta^{18}O$ (‰) | Rain (mm) | $\delta^{18}O$ (‰) |
| P1 | 3-hour | 299 | 335 | −8.4 | 413 | −14.0 |
| P2 | bulk | 327 | 279 | −8.9 | 333 | −14.7 |
| P3 | bulk | 321 | 336 | −8.6 | 398 | −14.2 |
| P4 | bulk | 342 | 378 | −8.8 | 338 | −14.4 |

## 2. Calibration and Simulation Performance

The best performance measures, KGE and the three perspectives of streamflow and $\delta^{18}O$ simulations are listed in Table S2. The streamflow simulations are satisfactory for all catchment-events. All $KGE_Q$ for the two catchments are higher than 0.85; the correlation ($r$) ranges from 0.87 to 0.97; the variability ratio ($V$) ranges from 0.93 to 1.06, and the bias error ($B$) ranges from 0.94 to 1.04. The $KGE_C$ simulations are also satisfactory ranging from 0.96 to 0.99 and 0.75 to 0.90 for PL and DL, respectively with PL better than DL. Note that event 5 in both catchments could not be simulated promisingly. Specifically, the individual performance of the three perspectives of KGE are at the similar level in the two catchments for $\delta^{18}O$ simulation.

**Table S2.** Best performance for simulating streamflow and $\delta^{18}O$. KGE and $V$, $B$, and r represent the Kling–Gupta efficiency coefficient, variability ratio, bias error, and correlation, respectively.

| Catchment-Event | Streamflow | | | | $\delta^{18}O$ | | | |
|---|---|---|---|---|---|---|---|---|
| | $KGE_Q$ | $V$ | $B$ | r | $KGE_C$ | $V$ | $B$ | r |
| PL01 | 0.924 | 0.993 | 0.975 | 0.928 | 0.966 | 0.999 | 1.001 | 0.966 |
| PL02 | 0.944 | 0.976 | 0.984 | 0.952 | 0.993 | 1.001 | 1.001 | 0.993 |
| PL03 | 0.921 | 1.057 | 1.039 | 0.962 | 0.964 | 0.998 | 1.001 | 0.965 |
| PL04 | 0.937 | 1.035 | 1.000 | 0.947 | 0.978 | 1.000 | 1.001 | 0.978 |
| PL05 | 0.938 | 0.965 | 0.983 | 0.952 | 0.608 | 0.998 | 1.012 | 0.608 |
| PL06 | 0.966 | 0.990 | 0.992 | 0.969 | 0.983 | 1.002 | 0.998 | 0.983 |
| DL01 | 0.885 | 0.954 | 0.935 | 0.917 | 0.900 | 0.931 | 0.996 | 0.929 |
| DL02 | 0.934 | 0.995 | 0.951 | 0.956 | 0.846 | 1.053 | 1.023 | 0.858 |
| DL03 | 0.851 | 0.926 | 1.025 | 0.873 | 0.749 | 1.139 | 1.020 | 0.792 |
| DL04 | 0.903 | 0.947 | 0.986 | 0.920 | 0.826 | 0.885 | 0.999 | 0.870 |
| DL05 | 0.933 | 0.975 | 0.978 | 0.941 | 0.731 | 0.943 | 0.989 | 0.737 |
| DL06 | 0.953 | 1.021 | 0.965 | 0.975 | 0.882 | 0.919 | 0.969 | 0.920 |

## 3. Compiled TRANSEP model results

We reviewed and summarized 64 events of 8 cases which used TRANSEP model to estimate $MTT_{ew}$ and $F_{ew}$ in different environments. Notably, basin area of these catchments is less than 8.8 $km^2$, lacking of meso-scale catchments. Rainfall amount in most cases are less than 101 mm, which is much smaller than our events (the lightest: 236 mm), except one event in WS10, Oregon (177 mm) and another one in Mack Creek, Oregon (155 mm). As for the duration of storms, most cases are shorter than one day except for the cases in Oregon which are comparable to our typhoons that usually last for two to three days. All average rainfall intensity is similar to our cases. $\delta^{18}O$ are used as tracer except in Johnson et al. (2007) who used dissolved $CO_2$ and in Mosquera et al. (2018) who used both $^{18}O$ and EC. The $MTT_{ew}$ and $F_{ew}$ range from 1.0 to 93.8 h and 0.04 to 0.77, respectively.

**Table S3.** Compiled TRANSEP model studies at a storm-scale.

| Site | Latitude | Area ($km^2$) | Slope (°) | Saturated hydraulic conductivity ($mm\ h^{-1}$) | Rainfall (mm) | Duration (h) | $RI_{avg}$ ($mm\ h^{-1}$) | Tracer | Transfer Function | $MTT_{ew}$ | $F_{ew}$ | Reference |
|---|---|---|---|---|---|---|---|---|---|---|---|---|
| Studies reporting both $MTT_{ew}$ and $F_{ew}$ | | | | | | | | | | | | |
| Steep catchments | | | | | | | | | | | | |
| K, Maimai, New Zealand | 42 | 0.17 | 34.0 | 250 | 27 | 13.0 | 2.1 | $^{18}O$ | EPM | 10.5 | 0.22 | Weiler et al. (2003) |
| | | | | | 70 | 30.0 | 2.3 | | TPLR | 10 | 0.18 | |
| Hillslope, HJ Andrews, Oregon | 44 | 0.002 | 27.0 | 450 | 31 | 61.8 | 0.5 | $^{18}O$ | GM | 15 | 0.22 | McGuire and McDonnell (2010) |
| | | | | | 60 | 82.5 | 0.7 | | TPLR | 14 | 0.06 | |
| WS10, HJ Andrews, Oregon | 44 | 0.102 | 37.0 | 450 | 177 | 107.5 | 1.6 | | TPLR | 28 | 0.11 | |
| | | | | | 31 | 61.8 | 0.5 | | GM | 8 | 0.27 | |
| | | | | | 60 | 82.5 | 0.7 | | TPLR | 34 | 0.10 | |
| Mack Creek, HJ Andrews, Oregon | 44 | 5.8 | 25.0 | 450 | 155 | 67.5 | 2.3 | $^{18}O$ | EM | 28.2 | 0.28 | Mosquera et al. (2018) |
| | | | | | 155 | 67.5 | 2.3 | | TPLR | 54.8 | 0.24 | |
| | | | | | 155 | 67.5 | 2.3 | EC | EM | 21.2 | 0.20 | |
| | | | | | 155 | 67.5 | 2.3 | | TPLR | 42.1 | 0.21 | |
| Gentle catchments | | | | | | | | | | | | |
| Upper Sabino, AZ | 32 | 8.8 | 7.0 | 0.33 | 26 | 3.0 | 8.7 | $^{18}O$ | EM | 4.5 | 0.23 | Lyon et al. (2008) |
| B1, Columbia | 5 | 1.59 | 8.7 | 36 | 24 | 4.5 | 5.3 | $^{18}O$ | TPLR | 26.1 | 0.23 | Roa-García and Weiler (2010) |
| | | | | | 38 | 4.8 | 8.0 | | | 1.5 | 0.24 | |
| | | | | | 30 | 2.8 | 10.9 | | | 25.7 | 0.32 | |
| B2, Columbia | 5 | 1.8 | 8.3 | 36 | 24 | 4.5 | 5.3 | | | 50.8 | 0.25 | |
| | | | | | 24 | 4.8 | 5.1 | | | 6.8 | 0.40 | |
| | | | | | 31 | 4.0 | 7.8 | | | 66.7 | 0.21 | |
| BB, Columbia | 5 | 0.62 | 10.1 | 36 | 16 | 3.3 | 4.9 | | | 3.3 | 0.12 | |
| | | | | | 21 | 3.8 | 5.6 | | | 5.3 | 0.27 | |
| | | | | | 16 | 3.8 | 4.3 | | | 14.4 | 0.14 | |
| SB, Canada | 46 | 0.07 | 7.7 | 180 | 14 | 1.2 | 11.8 | $^{18}O$ | TPLR | 7.6 | 0.33 | Segura et al. (2012) |
| AW, Canada | 46 | 0.11 | 13.0 | 180 | 25 | 10.3 | 2.4 | | | 1.2 | 0.77 | |
| | | | | | 14 | 1.2 | 11.8 | | | 11.9 | 0.29 | |
| | | | | | 38 | 2.4 | 15.9 | | | 1.7 | 0.52 | |
| | | | | | 7 | 2.9 | 2.4 | | | 4.4 | 0.28 | |
| VC, Canada | 46 | 0.11 | 8.4 | 180 | 14 | 1.2 | 11.8 | | | 1.5 | 0.55 | |
| | | | | | 38 | 2.4 | 15.9 | | | 1 | 0.42 | |
| YV, Canada | 46 | 0.3 | 11.0 | 180 | 25 | 10.3 | 2.4 | | | 33.4 | 0.32 | |
| | | | | | 14 | 1.2 | 11.8 | | | 31.3 | 0.42 | |
| SC, Canada | 46 | 0.38 | 10.3 | 180 | 25 | 10.3 | 2.4 | | | 16.1 | 0.31 | |
| | | | | | 14 | 1.2 | 11.8 | | | 1.2 | 0.36 | |
| | | | | | 38 | 2.4 | 15.9 | | | 12.9 | 0.52 | |
| | | | | | 7 | 2.9 | 2.4 | | | 7 | 0.40 | |
| PW, Canada | 46 | 0.48 | 8.9 | 180 | 14 | 1.2 | 11.8 | | | 26.6 | 0.34 | |
| | | | | | 38 | 2.4 | 15.9 | | | 1.1 | 0.60 | |
| | | | | | 7 | 2.9 | 2.4 | | | 26.3 | 0.19 | |
| EF, Canada | 46 | 0.91 | 9.2 | 180 | 14 | 1.2 | 11.8 | | | 3.1 | 0.30 | |
| | | | | | 38 | 2.4 | 15.9 | | | 31.4 | 0.47 | |
| | | | | | 7 | 2.9 | 2.4 | | | 12 | 0.21 | |
| LK, Canada | 46 | 1.47 | 9.0 | 180 | 25 | 10.3 | 2.4 | | | 93.8 | 0.51 | |
| | | | | | 14 | 1.2 | 11.8 | | | 11.7 | 0.33 | |
| | | | | | 38 | 2.4 | 15.9 | | | 4.7 | 0.52 | |
| | | | | | 7 | 2.9 | 2.4 | | | 60.3 | 0.23 | |
| Studies reporting $F_{ew}$ | | | | | | | | | | | | |
| Steep catchment | | | | | | | | | | | | |
| Veracruz, Mexico | 19.5 | 0.246 | 20.0 | 777 | 35 | 2.0 | 17.5 | $^{18}O$ | TPLR | - | 0.62 | Muñoz-Villers and McDonnell (2012) |
| | | | | | 23 | 2.0 | 11.5 | | | | 0.19 | |
| | | | | | 44 | 4.0 | 11.0 | | | | 0.34 | |
| | | | | | 31 | 9.0 | 3.4 | | | | 0.07 | |

| | | | | | | | | | | | | |
|---|---|---|---|---|---|---|---|---|---|---|---|---|
| | | | | | 101 | 4.0 | 25.3 | | | | 0.01 | |
| | | | | | 34 | 4.0 | 8.5 | | | | 0.12 | |
| Gentle catchment | | | | | | | | | | | | |
| Juruena, Mato Grosso, Brazil | 10.5 | 0.02 | 4.8 | 30 | 31 | 0.5 | 61.4 | Dissolved $CO_2$ | TPLR | - | 0.17 | Johnson et al. (2007) |
| | | | | | 20 | 0.8 | 26.7 | | | | 0.10 | |
| | | | | | 17 | 1.8 | 9.6 | | | | 0.32 | |
| | | | | | 5 | 1.3 | 3.8 | | | | 0.08 | |
| | | | | | 4 | 0.3 | 14.4 | | | | 0.15 | |
| | | | | | 28 | 2.3 | 12.4 | | | | 0.48 | |
| | | | | | 2 | 0.4 | 5.8 | | | | 0.05 | |
| | | | | | 11 | 0.6 | 18.3 | | | | 0.30 | |
| | | | | | 6 | 2.0 | 3.1 | | | | 0.14 | |
| | | | | | 15 | 0.8 | 19.5 | | | | 0.26 | |
| | | | | | 3 | 0.8 | 4.0 | | | | 0.04 | |
| | | | | | 11 | 0.8 | 13.3 | | | | 0.26 | |
| | | | | | 16 | 1.3 | 12.6 | | | | 0.27 | |
| | | | | | 15 | 0.4 | 34.8 | | | | 0.25 | |

## 4. Correlation between hydrometrics and model parameters

Correlation analysis reveals significant correlations between hydrometrics and the best-fit model parameters (Table S4). In the streamflow module, parameter $a_1$ and $a_3$ in loss function are negatively correlated to intensity-related hydrometrics, i.e., $RI_{avg}$, $P_{max3hr}$ and $Q_{max}$. Parameter $\alpha_q$ is negatively correlated to P, $P_{max3hr}$ and $Q_{max}$, but not correlated to average rainfall intensity. In the tracer module, both parameters in loss function are not correlated to hydrometrics. Shape parameter in event water transfer function ($\alpha_e$) is negatively correlated to intensity-related hydrometrics ($RI_{avg}$, $P_{max3hr}$ and $Q_{max}$). No significant correlation between $F_{ew}$ and all hydrometrics are found; however, $MTT_{ew}$ is negatively correlated to $RI_{avg}$ and $P_{max3hr}$. In sum, the intensity-related hydrometrics ($RI_{avg}$ and $P_{max3hr}$) are major controls on both streamflow and tracer modules.

**Table S4.** Pearson correlation coefficients between logarithmic hydrometric characteristics and logarithmic parameters for the storms. Values underlined and in bold are statistically significant with 95% and 99% level of confidence ($p < 0.05$ and $p < 0.01$), respectively.

| Parameter | P | D | $RI_{avg}$ | $P_{max3hr}$ | Q | $Q_{max}$ | $AP_{7day}$ |
|---|---|---|---|---|---|---|---|
| $a_1$ | −0.38 | 0.07 | −0.61 | **−0.76** | −0.23 | **−0.70** | 0.05 |
| $a_2$ | 0.10 | −0.03 | 0.17 | 0.35 | 0.05 | 0.33 | −0.04 |
| $a_3$ | −0.20 | 0.22 | −0.56 | -0.66 | −0.06 | −0.56 | 0.19 |
| $\alpha_q$ | **−0.70** | −0.47 | −0.37 | **−0.78** | −0.63 | **−0.75** | −0.40 |
| $\beta_q$ | 0.17 | **0.70** | −0.66 | −0.29 | 0.30 | −0.24 | **0.70** |
| $b_1$ | −0.44 | −0.45 | −0.04 | −0.49 | −0.28 | −0.44 | −0.45 |
| $b_2$ | 0.27 | 0.23 | 0.09 | 0.47 | 0.10 | 0.36 | 0.38 |
| $\alpha_e$ | −0.51 | 0.00 | **−0.71** | **−0.79** | −0.37 | **−0.76** | 0.02 |
| $\beta_e$ | 0.33 | 0.22 | 0.17 | 0.36 | 0.30 | 0.36 | 0.21 |
| $MTT_{ew}$ | −0.22 | 0.29 | **−0.68** | −0.54 | −0.07 | −0.49 | 0.30 |
| $F_{ew}$ | 0.08 | −0.32 | 0.52 | 0.28 | 0.14 | 0.29 | −0.23 |

## 5. Time-variant sensitivity analysis

Time-variant sensitivity analysis is used to imply the dynamics of rainfall-runoff generation in models. The parameter sensitiveness is generalized from 12-h moving windows Morris's μ into three segments. The Morris's μ are divided into three segments; they are rising, peak, and recession segments in accordance with hydrograph. The rising segment (seg. 1) is from streamflow rising to the peak flow; the peak segment (seg. 2) is from the peak to the inflection point of the recession; the recession segment (seg. 3) indicates the streamflow from the inflection to the end of the rainstorm. The Morris's μ in each segment is then averaged. Results of the three most sensitive parameter $\alpha_e$, $\alpha_q$ and $b_1$ are listed in Table S5. Compared among the three parameters, $\alpha_q$ and $b_1$ have a similar pattern,

in which the μ values ranking from high to low are seg. 2, seg. 3 and seg. 1. On the other hand, the μ value of $\alpha_e$ ranks from seg. 2, seg. 1 to seg. 3 in descending sequence. The storm magnitude does not have a significant effect on the μ values of the three parameters. Intriguingly, the highest μ value of $\alpha_e$ appears in seg. 1 during small rainstorms (event 2, 4 and 5) in DL. In sum, both shape parameters ($\alpha_q$, $\alpha_e$) play a predominant role in generating the quick flow, whereas parameter $b_1$ gets important during recession indicating rainfall partitioning regulates the runoff generation after the peak flow. Obviously, the sensitiveness of parameters varies with different segments, implying the necessity of time-variant parameterization.

**Table S5.** Morris's μ value of the sensitive parameters in the three segments of hydrograph in the catchment-events.

| Catchment Event | $\alpha_e$ | | | $\alpha_q$ | | | $b_1$ | | |
|---|---|---|---|---|---|---|---|---|---|
| | **seg. 1** | **seg. 2** | **seg. 3** | **seg. 1** | **seg. 2** | **seg. 3** | **seg. 1** | **seg. 2** | **seg. 3** |
| PL01 | 15.2 | 32.2 | 5.8 | 5.8 | 25.6 | 21.9 | 8.6 | 16.9 | 38.2 |
| PL02 | 31.8 | 68.3 | 20.1 | 44.2 | 172.7 | 101.1 | 5.1 | 20.3 | 28.7 |
| PL03 | 39.8 | 65.1 | 8.3 | 8.1 | 47.4 | 35.1 | 12.4 | 31.7 | 61.5 |
| PL04 | 18.1 | 14.4 | 6.1 | 6.6 | 20.5 | 19.9 | 11.8 | 20.8 | 29.3 |
| PL05 | 4.7 | 13.3 | 1.1 | 1.2 | 3.5 | 3.9 | 3.7 | 4.5 | 9.3 |
| PL06 | 158.2 | 172.1 | 7.8 | 94.2 | 205.1 | 55.1 | 14.4 | 24.6 | 23.9 |
| DL01 | 12.0 | 17.6 | 4.0 | 3.5 | 14.6 | 14.3 | 12.3 | 14.5 | 30.1 |
| DL02 | 44.1 | 37.5 | 5.0 | 38.6 | 83.2 | 36.8 | 2.9 | 14.5 | 25.3 |
| DL03 | 29.6 | 42.4 | 8.6 | 9.8 | 46.1 | 35.6 | 15.9 | 25.8 | 54.0 |
| DL04 | 34.5 | 13.0 | 6.4 | 9.3 | 26.6 | 23.8 | 11.2 | 18.7 | 29.3 |
| DL05 | 21.5 | 13.1 | 1.2 | 9.4 | 16.1 | 7.3 | 14.7 | 15.9 | 14.9 |
| DL06 | 128.5 | 148.1 | 3.8 | 68.7 | 164.2 | 38.6 | 10.8 | 20.2 | 20.4 |